SKA1-LOW CONFIGURATION – CONSTRAINTS & PERFORMANCE ANALYSIS

Document number SKA-TEL-SKO-0000557
Document Type ..... REP
Revision 01
Author ..... P. Dewdney, J. Wagg, R. Braun, W. Turner
Date 2016-05-31
Document Classification ..... FOR PROJECT USE ONLY
Status ..... Released

Name	Designation	Affiliation	Signature	
Additional Authors:				
P. Dewdney	SKA Architect	SKAO	Peter Dewdney	
			Date:	Jun 22, 2016
Owned by:				
P. Dewdney	SKA Architect	SKAO	Peter Dewdney	
			Date:	Jun 22, 2016
Approved by:				
A. McPherson	Head of Project	SKAO		
			Date:	Jun 22, 2016
Released by:				
A. McPherson	Head of Project	SKAO		
			Date:	Jun 22, 2016

DOCUMENT HISTORY

Revision	Date Of Issue	Engineering Change Number	Comments
A	2015-05-15	-	First draft release for internal review
01	2016-05-31	-	First release

DOCUMENT SOFTWARE

	Package	Version	Filename
Wordprocessor	MsWord	Word 2007	SKA-TEL-SKO-0000557_01_ DesignConstraints
Block diagrams			
Other			

ORGANISATION DETAILS

Name	SKA Organisation
Registered Address	Jodrell Bank Observatory Lower Withington Macclesfield Cheshire SK11 9DL United Kingdom Registered in England & Wales Company Number: 07881918
Fax.	+44 (0)161 306 9600
Website	www.skatelescope.org

TABLE OF CONTENTS

LIST OF FIGURES

LIST OF TABLES

LIST OF ABBREVIATIONS

EoR .....Epoch of Reionisation
CD .....Cosmic Dawn
FWHM .....Full Width Half Maximum
HPSO .....High Priority Science Objective
PSF .....Point Spread Function
RFI.....Radio Frequency Interference
RMS .....Root Mean Square
SEFD.....System Equivalent Flux Density
SKA .....Square Kilometre Array
SKA1 .....SKA Phase 1
SKAO .....SKA Organisation

1 Introduction

1.1 Purpose of the document

A calibration consultation meeting, held on Feb. 25, 2016 [RD3] [RD4], discussed the suitability of the 'V4D' configuration for SKA1-low, an evolution of the 'V4A' configuration in [RD1].

Previous calibration-consultation meetings held in April and December 2015 resulted in the following aspects of the SKA1-low array configuration (see Figure 1):

1. The locations of the outer stations, which lie outside the SKA1-low Central Area.
2. A circular area (SKA1-low "Central Area") around the core of the SKA1-low array, within which the final array was left to be defined.

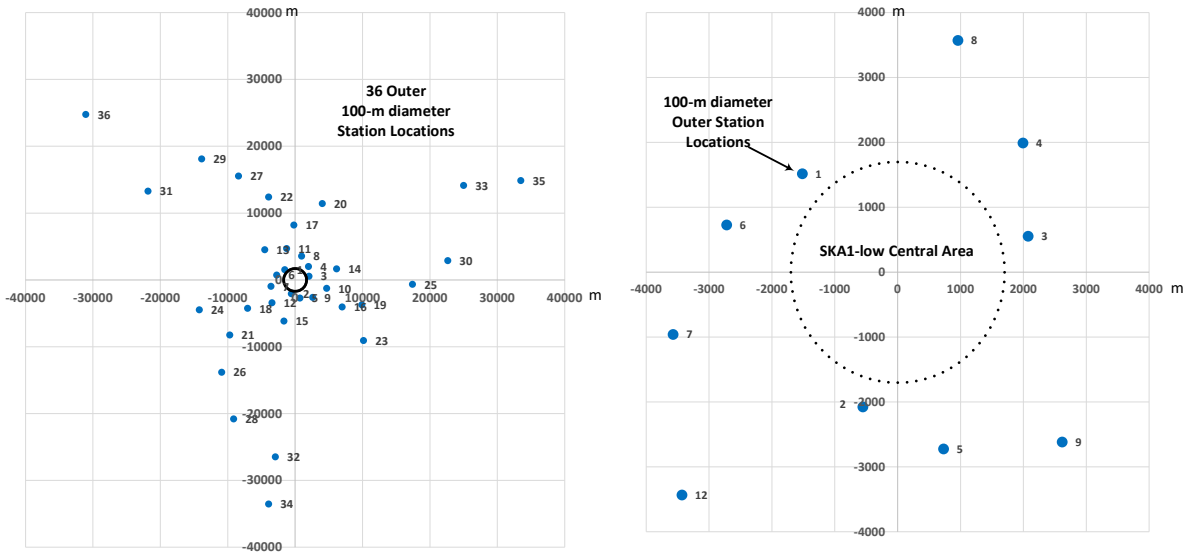

Figure 1: Left: The location of the outer stations defined in [RD2]. **Right:** The central region for which the configuration was undefined in Dec. 2015 [RD4]. **Note that the numbers in this diagram are no longer in use (see [RD13]).**

The purpose of this follow-on analysis is to take into account in-place constraints (e.g. the results shown in Figure 1), key results of the meeting on Feb 25, 2016 (e.g. the need for very low spatial-frequency coverage) and some subsequent simulations, and then to propose an array configuration for the Central Area as well as the configuration of antenna-elements within stations.

A second purpose is to carry out an end-to-end impact analysis of the new configuration, including support of a large number of 'virtual substations', again under conditions of overall cost constrained to approximately to present values.

1.2 Scope of the document

Within the scope is consideration of the three main science areas for which the telescope is primarily being designed:

1. EoR/CD (power spectrum and deep line imaging),
2. Pulsar search and timing,

3. Standard imaging[1].

2 References

The following documents are referenced in this document. In the event of conflict between the contents of the referenced documents and this document, **this document** shall take precedence.

[RD1] SKAO science team, 'SKA1 LOW configuration memo v4A', 2015.
[RD2] P. E. Dewdney, 'SKA1-low Configuration Coordinates', Dec. 15, 2015.
[RD3] P. Dewdney, J. Wagg, R. Braun, M.-G. Labate, 'Objectives for a Proposed SKA1-Low Station-Configuration Workshop', Feb 1, 2016.
[RD4] J. Wagg, 'Summary of the Third SKA1-low Calibration Consultation Workshop', Mar. 1, 2016.
[RD5] Mellema, et. al., 'White Paper on Reionization and the Cosmic Dawn with the Square Kilometre Array', Sept. 13, 2012.
[RD6] SKA Science Review Panel, C. Carilli et. al., 'Final Report Science Review Panel', Feb 5, 2015.
[RD7] S. J. Wijnholds and J. D. Bregman, 'Calibratability by Design for SKA's Low Frequency Aperture Array', 2014.
[RD8] P.E. Dewdney, W. Turner, R. Millenaar, R. McCool, J. Lazio, T. J. Cornwell, "SKA1 System Baseline Design", SKA Document SKA-TEL-SKO-DD-001, Mar 12, 2013.
[RD9] T. J. Cornwell, 'SKA1-Low Array Configuration', SKA-TEL-SKO-0000000-AG-CNF-LOW (draft), July 7, 2015.
[RD10] M. Bendotti, 'SKA-TEL-INAU-0000042 – Draft Cost Report', Sept. 11, 2015.
[RD11] K. Zarb Adami, 'Low Frequency Aperture Array, Signal Processing Specific and Overall Design Report', SKA-TEL.LFAA.SP.MGT-AADC-R-002, Oct. 31, 2014.
[RD12] R. Braun and P. Dewdney, 'SKA Array Configurations', SKA-OFF.AG.CNF-SKO-TN-001, Rev 1, May 16, 2014.
[RD13] P. Dewdney and R. Braun, 'SKA1-low Configuration Coordinates – Complete Set', SKA-TEL-SKO-0000422, Rev 2, May 1, 2016.
[RD14] R. Perley and B. Clark, 'Scaling Relations for Interferometric Post-Processing', EVLA Memo 63, Sept. 2003.
[RD15] 'NIMA TR8350.2, Department of Defence World Geodetic System 1984', 3rd Edition Amendment 1, 3 January 2000.

3 Definitions

The following definitions are used for consistency in describing the configuration of SKA1-low:

Station

A circular array of antenna elements that has a clear physical boundary, whose output signals are connected individually to the SKA1-low beam-former.

Station diameter

The diameter of a circle that is a best-fit circle to the outer boundary of the array of antenna elements that make up a station.

Substation

[1] Note that an imaging capability is also required for spectral-line imaging of the EoR/CD signature, a critical part of this science.

An array of adjacent antenna elements contained within a station which can be beam-formed to produce a data-stream that can be correlated. Sometimes referred to as a virtual station.

Superstation

A group of stations in close proximity or even sharing a boundary which can be beam-formed to produce a data-stream that can be correlated.

Correlatable Entity

A station, substation or superstation which has been beam-formed to produce a data stream to be correlated.

Sparse-dense Transition Frequency

The frequency at which the antenna elements in an array are $\lambda/2$ apart on average.

Central Area

An area 1700 m in radius with a centre at the centre of the array.

Core

An area 1000 m in diameter within which the individual stations are randomly located with no overlap.

Cluster location

The position of a cluster outside the core area. Positions are defined in the WGS84 coordinate system.[2]

Cluster

A group of six stations placed randomly around a cluster location, defined for stations outside the core area. The value of six arises to provide sufficient collecting area over the range of interferometer spacings outside the core (see Sections 5.4.6, 5.4.7 and 7).

Cluster diameter

The diameter of the area within which individual station belonging to the cluster are located.

4 A Brief Description of SKA1-low and Its Array Configuration

Previous proposals for SKA1-low configurations can be found in [RD1], [RD2], [RD4], [RD8] and [RD12] and references therein. As noted in the introduction, a series of meetings were held to provide guidance and input to the design. The present document presents a version which takes into account this input to the extent possible while satisfying constraints of cost, previous commitments, and existing design work.

In summary, the configuration analysed here consists of the following and shown in Figure 2:

- A set of 512 stations of 35-45 m in diameter.
- There are 256 antenna elements within each station, which are in randomised positions.[3]
- Clusters of 6 stations in the locations shown in Figure 1.
- A core of 224 stations randomly distributed over circular area of 1000 m diameter.
- Additional clusters of 6 stations forming a continuation of the spiral arms inside the central area.

[2] WGS84 is an Earth-centred, Earth-fixed terrestrial reference system and geodetic datum [RD13].

[3] As well as this, there will have to be sufficient space around the antenna elements to access them for servicing (see [RD1] for explanation).

- Clusters are 100-150 m in diameter, and the positions of individual stations within clusters are randomised.

A more detailed description of the physical location of each station can be found in [RD13].

The array is serviced by a central processing facility located near the central area, as well a series of huts located near the clusters of stations. Each antenna element contains a low-noise amplifier and drives an analogue signal over optical fibre either the central processing facility or a hut. Both the huts and the central processing facility contain station beam-forming equipment for the stations connected to them. Station beam-formed signals from the huts are transmitted via digital signals over fibre to the central processing facility. Station beam-formed signals are also sent to the SKA1-low correlator-beamformer, which performs both correlation and array beamforming. The correlator-beamformer will likely also be located in the central processing facility. More detail can be found in [RD11].[4]

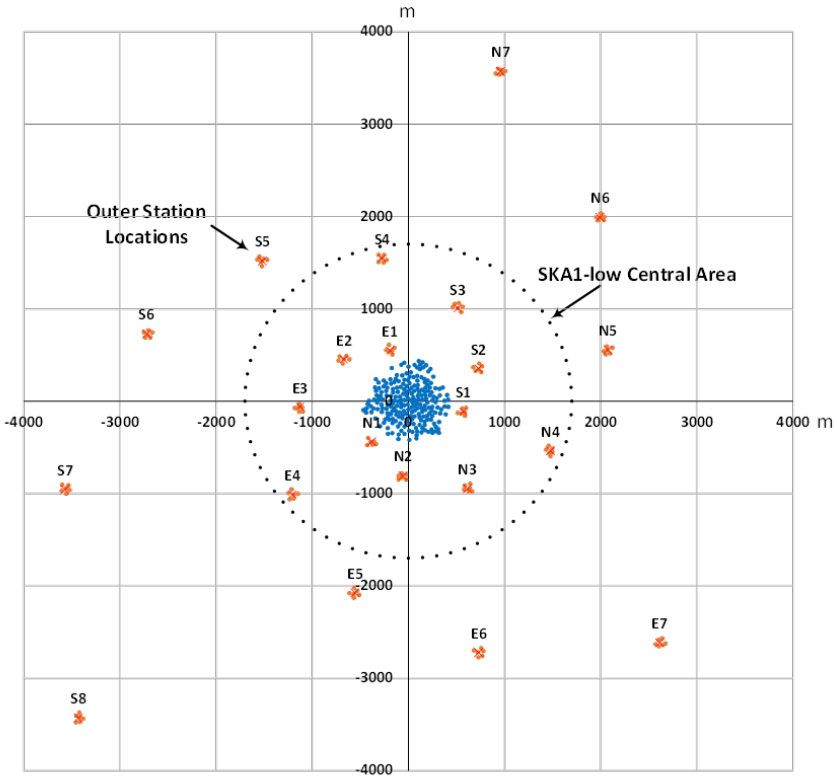

Figure 2: The inner part of the array configuration described herein (from [RD13]).

5 Constraint and Impact Analysis

This section contains a summary of previously established aspects of the SKA1-low system and array configuration, as well as additional aspects that arose in the Configuration Consultation meeting of Feb. 2016. They are considered in the following categories:

1. Physical and cost constraints.
2. Primary frequency ranges of interest.
3. Ionospheric calibration.
4. Distribution of collecting area in the array.

[4] Note that the purpose of this document is not to describe the precise locations of processing equipment (huts, central processing facility, correlator-beamformer). These will be located so as to provide optimised service to the array.

5. Distribution of collecting area within a stations and the core.
6. Beamforming architecture.
7. Correlator architecture.
8. Compute scaling.

Some of the items in the following sections are hard constraints and others are science-driven goals within the three science areas: EoR/CD, pulsars, standard imaging. The list contains a mixture of agreed constraints (major aspects of the array configuration, size/cost of beam-former, size/cost of correlator) and science goals that have arisen from recent 'calibration consultation' meetings. Only aspects of the system that affect the configuration of antennas or are affected by the configuration are considered.

5.1 Physical and Cost Constraints

- The antenna-array must be located within the Boolardy station.
  - This limits the maximum baseline to ~65 km.
- The core location has been fixed by terrain analysis:
  - The ground is flat, relatively free of flooding, etc.
  - This puts constraints on a configuration of stations that also meets goals derived from astronomical needs.
- A full 2D configuration would be better for snapshot imaging, but it is very expensive.
  - A 2-D configuration, 'RB45', described in [RD9] had previously been analysed to obtain a cost [RD10]. The difference for infrastructure alone between RB45 and a spiral-arm configuration similar to that discussed in this document is more than 20 MEuro.
  - The next logical step is to maintain the desired radial profile of collecting area, but aggregate stations in groups. A configuration consistent with items a-c is documented in [RD2].
- The total available number of antenna elements is 131,072. This number is the result of an earlier costs analysis, which then resulted in the 're-baselined' definition of the size of SKA1-low.
- As noted in Section 1.1, the locations of outer stations has been agreed (those outside a radius of 1.7 km from the centre).
  - Each of the locations will contain one or more arrays of antenna elements (stations) within a diameter of 100-150 m.[5]
- The beamformer as currently costed must not increase in overall size or cost.
- The correlator as currently costed must not increase in overall size or cost.
- Science Data Processing is not constrained in this document, since its current cost and design is uncertain.

5.2 Primary Frequency Ranges of Interest

The most important frequency range for the three main science areas:

- EoR/CD:
  - Power-spectrum observations: 50 – ~200 MHz, possibly as high as 250 MHz.
  - Imaging observations: 100 – ~200 MHz.
- Pulsars: 150 – 350 MHz.
- General imaging: 50 – 350 MHz (higher frequencies for deep continuum imaging, where the confusion limit is lower).

[5] This range has been inserted to accommodate the possibility of a larger antenna element than the present version.

5.3 Calibration observations of ionospheric effects

- A distribution of collecting area that permits imaging of the 'shifted positions' of sources over the field-of-view as a function of time due to ionospheric fluctuations.
    - It has been shown in [RD7] that sufficient signal-to-noise ratio can be obtained from single 35-m diameter stations at each of the outer-array locations. While [RD7] suggests that 50 stations distributed homogeneously over a 70 km area, the array configurations discussed here have more stations distributed in clusters. The authors have since suggested that this also should be sufficient (see [RD4] and references therein).
    - This would cover only the field-of-view of a 35-m station. If larger fields-of-view are needed then multiple beams would be needed or sub-station configurations on all baselines.
- Images of sources in the field need sufficient resolution to calibrate the system, accurate foreground characterisation, both of which assist in calibrating the ionosphere as well (see Appendix 3 in [RD6]).
    - A maximum baseline of ~65 km is sufficient [RD6].
- A sufficiently uniform distribution of pierce points is available from observations to be able to reconstruct the ionospheric phase screen [RD7].
- Quasi-continuous observing with full resolution is needed to calibrate ionospheric effects, which vary on timescales of ~10 seconds.
    - Even if science data will be collected only from short baselines in the central part of the array, interferometer data from the outer array will be needed continuously.

5.4 Distribution of collecting area in the array

5.4.1 Pulsar Observations:

- The highest sensitivity for pulsar observations is obtained by providing as much collecting area as possible in a tight core.

5.4.2 EoR/CD Imaging (Tomography)

- The highly red-shifted HI line is extremely weak and distributed over the field; thus they are considered brightness-temperature limited. Highest sensitivity is obtained at low resolution.
- The ideal array contains as much collecting area as possible in an array out to ~1 km radius.

5.4.3 EoR/CD Power Spectrum

- *High-fidelity* measurements of very low-order *u-v* spacings are required, implying that spacings of the order of 10 m are required. The best results are obtained by cross-correlating stations that are ~10 m in diameter (see [RD4] and references therein).
- Systematic errors and estimation limits have to be considered in k-space ([RD5], [RD4] and references therein), which can be split into two components, $k_{\perp} \propto b/\lambda$ and $k_{/\!/} \propto 1/B$, where b is interferometer baseline, λ is wavelength, and B is bandwidth. While error analysis is outside the scope of this paper, it can be said that complete coverage of *b* in the range from 10's to 100's of meters with sufficient signal-to-noise ratio is critically important for detecting the EoR signal in k-space.

5.4.4 EoR/CD general

- It has been noted that the 're-baselined' number of elements is likely to be at a critically low boundary, depending on how many antenna elements can be placed within the ~1 km radius.
- 'Foreground subtraction' of continuum sources will be required (see below).

5.4.5 *u-v* Coverage

- The typical practical tracking range with these aperture arrays is ±2 hr.
- The array configuration has been configured as spiral arms with triplets of stations rotated around the centre to improve u-v coverage for short observations.

5.4.6 Continuum Imaging

- Standard imaging: A smooth, scale-free radial profile of collecting area beyond the core, out to the maximum baseline, has been adopted.
    - Avoids favouring particular spatial frequencies in images.
    - Much longer baselines would be needed to avoid source confusion at all SKA1-low frequencies, but this is not possible currently. However, reasonably long integration times are possible at the high end of the band before the confusion limit is reached.
- Foreground subtraction for EoR/CD: Relatively high-resolution (full range of baselines) imaging is needed, with good *u-v* coverage, similar to that needed for general imaging, but in this case emphasis on calibration.
    - Confusion, per se, does not prevent foreground subtraction, but may have implications for image fidelity. Excellent calibration will be needed to subtract the foreground with sufficient accuracy, especially calibration of instrumental polarisation [RD6].

5.4.7 Spectral Line Imaging

- Standard Imaging:
    - Same basic requirements as for continuum imaging.
    - Spectral line images tend to have diffuse emission, which requires good coverage in short spacings.

5.5 Distribution of collecting area within stations and the core

5.5.1 General Constraints

5.5.1.1 Randomisation of Antenna-Element Positions

- Placement of antenna elements must be randomised and not on a regular grid.
    - A regular grid of antenna elements will generate station beams that exhibit 'blind spots', a well-known electromagnetic phenomenon.
    - Randomisation implies a certain amount of room between antenna elements. This decreases the sparse-dense transition frequency, decreases the filling-factor and increases the station size, given a fixed number of antenna elements.
    - There will have to be sufficient space around the antenna elements to access them for servicing.

5.5.1.2 *Sparse-Dense Frequency Transition*

- The opposing impacts of the sparse-dense transition frequency.
    - A low transition frequency will mean that the filling factor at high frequencies will be low.
    - A high transition frequency will mean that the effective collecting area will be fixed over a large fraction of the frequency range, while the sky noise rises rapidly at the low end of the band.
        - Collecting area above the transition frequency scales as λ^2; below, collecting area is fixed, whereas sky noise increases as $\lambda^{\sim 2.55}$.

5.5.1.3 *Factors affecting sensitivity*

- Utilisation of antenna elements at full weight.
    - In general favours physical station configurations, rather than virtual,
- Sensitivity in the core for 35-m diameter scales (~100 MHz) is at a critical point – cannot afford to reduce the size of the core.
    - Indicates the use of 35-m diameter physical stations in the core.

5.5.1.4 *Shared Signals*

- Correlatable entities may not contain signals from shared antenna elements.
    - Generates spurious autocorrelation components in the cross-correlations between correlatable entities.
    - Does not prevent the use of shared antenna elements, just correlation of the stations for which they are shared.

5.5.1.5 *Tapering*

- Station beams formed as a weighted sum of signals from antenna elements can produce beams with lower near-in sidelobes.
- However, there is significant signal-to-noise penalty for 'heavy' weighting. There can also be a higher far sidelobe level since there are fewer "effective antennas" per station.
- Weighting by physically 'sparsing' the antenna elements can achieve the same goal at a specific frequency, but it is not flexible enough to be used over very wide bands.
- Tapering that is irreversibly part of the architecture, such as sparsing the antenna elements will not be used.

5.5.2 EoR/CD observations

5.5.2.1 *EoR/CD sample variance and science field-of-view*

- Sample variance is inversely proportional to the 'volume' derived from the size of an image cube at a selected redshift range.
- Volume, hence sample variance, scales with size of the science field-of-view; for 21 cm EoR/CD power spectrum studies sample variance in *k*-space decreases as field-of-view increases as it is determined by the number of independent measurements of a given *k*-mode. Increased field-of-view can be achieved in two ways: decreased station size or multiple simultaneous beams.
    - Large stations with multiple beams are clearly superior for decreasing sample variance. (But note that large stations cannot capture the very short spacings that are required for power-spectrum observations).

- The SKA1-low design will permit trading bandwidth (number of channels) with beams, and possibly numbers of stations correlated (see below). There are likely to be astrophysical reasons to limit extreme versions of these trades (e.g. very small fields-of-view but very large bandwidths or the other way around).

5.5.2.2 Single-beam field-of-view for tomography observations

- Based on recommendations derived in [RD5], a minimum of 20 deg^2 on the sky at ~100 MHz is needed for both cosmic dawn and imaging (tomography).
- This implies a station of ~35-m in diameter. This size has been re-examined over several years (e.g. [RD5]) and is widely accepted.
    - Nevertheless, 35m stations make a beam that is potentially too small to image low redshift bubbles (i.e. at high frequencies).
- With a total of 131,072 antenna-elements available, 512 stations can be populated with 256 antenna-elements each.
- The resulting area allowed for each antenna is approximately 3.8 m^2.
- The actual diameter of the antennas is 1.2 m, leading to a filling factor of ~0.4.[6] This provides room around the antennas for randomising the positions.
- Antenna elements may have to be increased in physical diameter in order to adequately cover the low-frequency part of the band. The expected effect is a modest increase in station diameter (~10 %). However, this has not yet been substantiated.

5.5.2.3 Single-beam field-of-view for power-spectrum observations:

- As noted in item 5.4.3 above, there is a strong case for a station size of ~10 m in diameter to obtain high-fidelity measurements of very short *u-v* spacings.
    - The ability to measure large-scale information (short spacings) cannot be replicated by multi-beaming and mosaicking to obtain a similar field-of-view similar to that for a 10-m diameter station.
- Stations of this size will be needed only in the core, and must be close-packed.
- 10-m diameter apertures can be implemented as sub-stations (virtual stations) of the 35-m diameter stations in the core.
- Ideally as much collecting area in the array should be configurable as sub-stations and correlated as possible, with emphasis on the core.
- A single 35-m diameter station can be filled with as many as 7 sub-stations, if they are packed optimally. The utilisation efficiency[7] for antenna elements would be 78% in this case. More conservatively, with 6 sub-stations, the utilisation efficiency is 67%.

5.5.3 Standard Imaging

- No particular issues arise in standard imaging using 35-m diameter stations. However, any requirement for imaging of the largest, most diffuse sources would benefit significantly from direct measurement of 10-m baselines (e.g. the continuum cosmic web).
- Station beams must be the same diameter for all stations to achieve high-dynamic range images.
- No science requirement has been identified for super-stations.
- There is an argument for superstations, based on reducing the amount of computing required for imaging smaller fields-of-view. However, superstations produced as a geometric patterns

[6] The version at the SKAO in Manchester is 1.2 m across the widest point. This may not be the current version.

[7] Utilisation efficiency refers to the fraction of antennas in a station that are used in forming the beam from any substation. It amounts to the maximum fraction of area contained in circles packed into a larger circle, where the diameter ratio is 3.

of stations (e.g. see [RD1]) may introduce structured side-lobes in the synthesised beam that also imply additional computing effort. A significant simulation effort would be needed to decide which is better, and since there is no direct science or calibration requirement, this cannot be pursued.

5.5.4 Pulsar and Transient Observations

- No particular issues arise in pulsar observations using 35-m diameter stations.
- Highly dispersed transients, such as those detected at the output of the de-disperser would be similarly unaffected.
- Multi-beaming and the general flexibility of the architecture will be useful for various types of transient-detection observations.

5.6 Beamforming Architecture

In this section a method is developed to assign as much flexibility of usage to the beam-forming architecture without significantly changing its overall cost. Assumptions and approximations are needed, designed to capture the overall performance of the beam-forming system as it is currently designed and costed, but which may not precisely mirror the current design in detail.

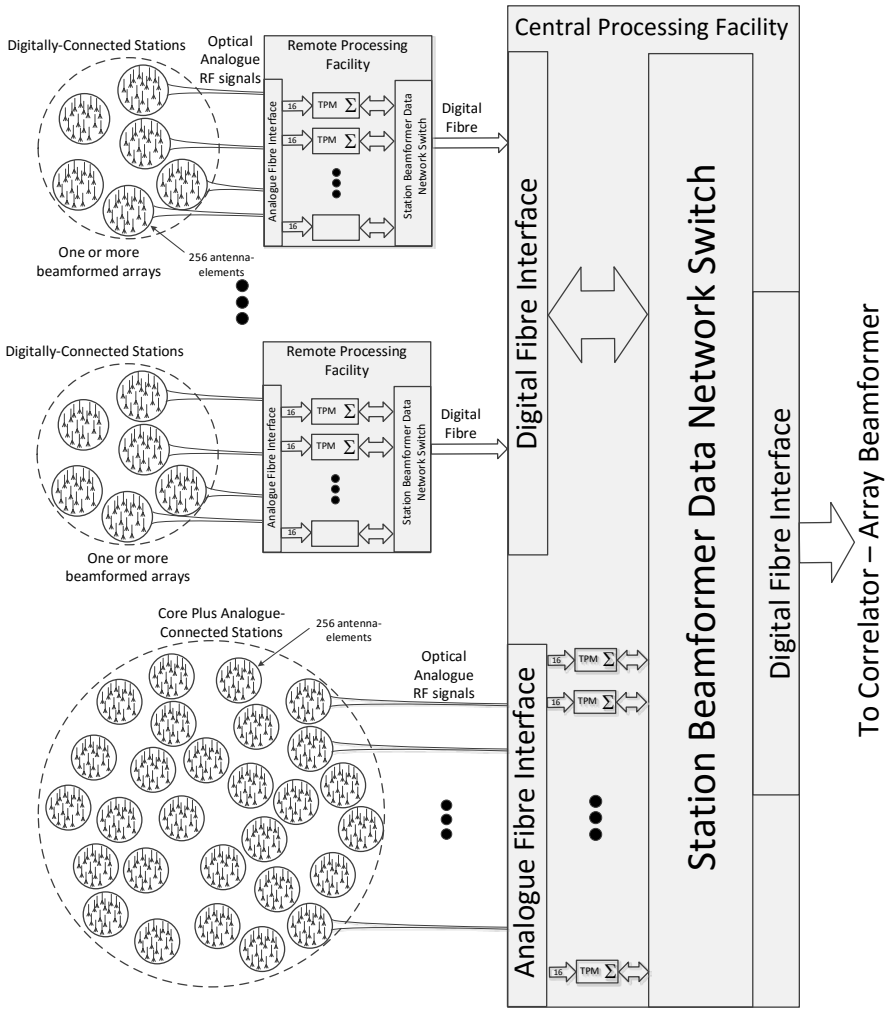

Figure 3: An overview system diagram showing the arrays of antenna-elements (left) that are connected via analogue signals and those connected by digital signals, with emphasis on the architecture of the beam-former (right).

Figure 3 is a top-level view of the SKA1-low array with emphasis on the beam-forming function. The actual locations of the arrays of antenna elements (stations) are provided in [RD13].

The overall function of the beam-former is to digitise analogue signals arriving from each antenna-element in two polarisations, and to form output data-streams, consisting of a weighted vector-sum from a selection of signals from the antenna-elements. The weights are designed to 'point' the beam in a particular direction, to apply calibrations, and to apodise the aperture. This is to be done with a degree of real-time programmability sufficient to carry out the science. There is no specific implication of the number of antenna-elements involved in a particular beam-sum, but there will be practical limitations.

5.6.1 Remote Processing Facilities

The ratio of the number of Remote Processing Facilities to the number of clusters cannot be defined in this document (i.e., it is not the intention of Figure 3 to do so). Determination of this ratio will require a cost study to obtain an optimum number of clusters serviced by each Remote Processing Facility. It is expected that the study will take into account the capital cost of the shielded buildings, provision of power and connectivity, access roads, etc.[8] For example, near the core it may make sense to aggregate Remote Processing Facilities so that they service multiple clusters. However, it is anticipated that the minimum number of stations serviced by a Remote Processing Facility will be six in a cluster. The data-rate emanating from a cluster is discussed in Section 5.6.3.3.

5.6.2 Current Beam-former System Design

This description is based mainly on the baselined version of the architecture as of Jan. 26, 2015 [RD11]. It is mainly an abstraction of the aspects of the architecture that affect or proscribe the system design and/or the flow-down from recent definitions of the SKA1-low array configuration.

Figure 4 shows a generalised form of the architecture, with some significant details of how the main parts are organised. Note that as shown in Figure 3, some of the groups of tile processors shown in Figure 4 will be located in the Remote Processing Facilities.

[8] The maximum distance traversable by analogue fibre directly from antenna elements may also influence results of the study, although there will be a risk that long analogue fibre systems will have to be sufficiently gain-stable (complex gain). This in itself may have to be established under real operational conditions.

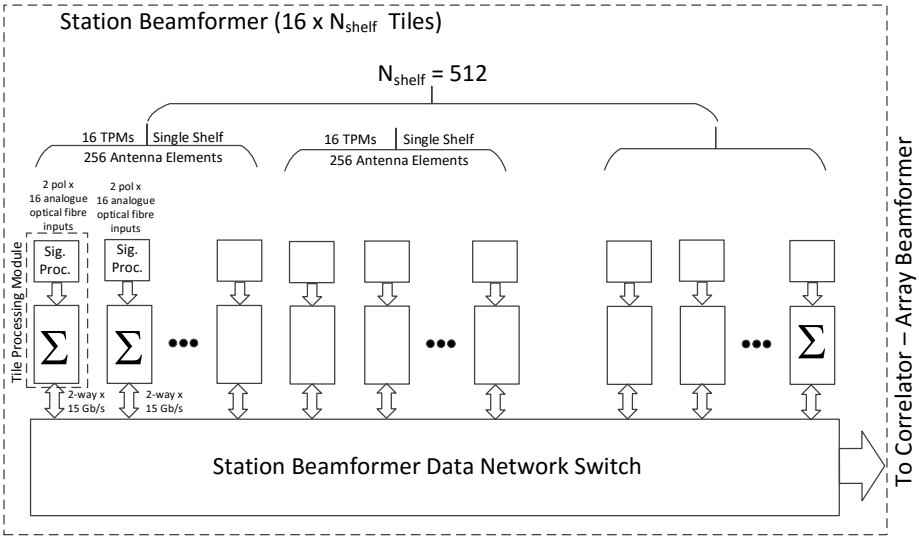

Figure 4: The general form of the beam-former system, showing important aspects of the granularity of the architecture.

5.6.2.1 Tile Processor Module

- The tile processor module is the device whose main functions are:
  - receive analogue optical signals from the antenna-elements,
  - digitise analogue signals,
  - channelise the incoming signals,
  - apply calibration coefficients (including polarisation rotation),
  - apply appropriate phases to point the beam,
  - sum the resulting signals to form a partial beam-sum.

5.6.2.2 Granularity

- The architecture supports beamforming in quanta of 16 (dual-pol'n) antenna-elements, enabled by a single 'tile processing module' (see Figure 4).
  - Partial sums are formed, which can be combined with other partial sums to form complete beams.
  - In principle, partial sums of fewer than 16 antenna-elements can be formed, but this leads to inefficient use of tile processing modules.

5.6.2.3 Beam-bandwidth Product in the Tile Processor Module

- The beam-former capacity for each tile processor module is limited mainly by a beam-bandwidth product.
  - The 300 MHz science bandwidth is sampled at 800 Msamp/s (i.e., f_s = 800 MHz, where f_s is the sample frequency). The sampled band (400 MHz) is processed into 512 frequency channels, yielding a channel bandwidth of 781 kHz. The science bandwidth of 300 MHz is divided into up to 384 frequency channels.
  - Thus the channel-beam product, $N_b N_{cc}$ is constant at 384, where N_b is the number of beams and N_{cc} is the number of (coarse) channels. N_{cc_max} = 384.
  - By design, the maximum number of beams is 8, which implies that at least 48 channels are available for each beam.
  - A single station beam formed from 256 antenna elements over the full RF bandwidth will require a sum of 16 partial beam-sums, which utilises 16 tile processor modules

to full capacity. As noted above, if the beam-bandwidth product remains constant, more beams can be produced.

- Each beam-sum results in a data-stream that is passed on to the correlator.
  - The nominal output data rate in a beam-sum is: $R_d = 2\ B\ N_p n_{bs} k_{os}$, where the factor of 2 is the Nyquist factor, *B* is bandwidth (Hz), N_p is the number of polarisations (2), n_{bs} is the sample-word-width (bits) and k_{os} is an oversampling-factor (32/27). For the full bandwidth, this comes to 300 x 10^6 x 2 x 2 x 8 x (32/27) = 11.4 Gb/s (see also Section 5.6.3.1).
  - This rate is independent of the number of partial beams included in any beam-sum.

5.6.3 Beam-former Performance-Product

5.6.3.1 Station-Channel-Beam Trade Space

- System performance is characterised by the maximum total output data rate, which is taken as the 'beam-former performance-product'.
- $P_{bf} = r_b N_s N_b N_{cc} \frac{300}{384}$, where r_b is a constant to convert MHz to Mb/s, N_s is the number of stations, N_b is the number of beams, and N_{cc} is the number of (coarse) channels. $r_b = 10^6\ x\ 2\ x\ 2\ x\ 8\ x\ \left(\frac{32}{27}\right) = 37.9$ Mb/s for both polarisations. P_{bf} is constant, while the numbers of channels, beams, and stations can be varied within limits. $P_{bf} = 5.8\ x\ 10^6$ Mb/s.
- By design, N_{cc_max} = 384 and N_{b_max} = 8.
- Since N_{s_max} = 131072/16 = 8192, limited by the granularity of the tile processors, the $N_{cc} \cdot N_b$ product is 24 at N_{s_max}[9]. Therefore, even with 8 beams, N_{cc} = 3. This means that the beam-former can support at least 3 coarse channels for any combination of beams and stations.
- Note that limit on the number of stations does not apply to the present design of the correlator (see Section 5.7.1). The correlator performance product will account for the number of baselines processed, which is proportional to N_s^2.

5.6.3.2 Output Data-Rate

- For 512 stations, the total data-rate is 11.4 Gb/s x 512 (35-m diameter stations) = 5.8 Tb/s (nominally 10 Tb/s).
- These will be made available on the outputs of a data-switch with 40 or 100 Gb/s capacity.
- The maximum that could be produced in principle for a single beam per station[10] is (131072/16) x 11.4 Gb/s = 93.4 Tb/s. However, it not expected that the data-switch could handle this total bandwidth nor could the correlator system.
- Figure 5 shows an implementation of the data-switch, based on [RD11]. The figure indicates the degree of locality in the actual assignment of the connections so as to avoid too much traffic passing through the Aisle Switches. In a station-beam-channel trade there may be limitations resulting from how data-streams are transmitted to the correlator (e.g. for a given number of physical ports, packets may contain data from different station/channel/beam combinations). The granularity of how packets are assigned to physical channels may affect the details of the interface with the correlator. This aspect is outside the scope of this document; however, there is considerable design flexibility to handle many combinations of beams, channels and stations.

[9] $N_b N_{cc} = \frac{P_{bf}}{8192\ r_b} \frac{384}{300}$

[10] Where in this case a station is actually 16 antenna-elements beam-formed in a single tile-processor module.

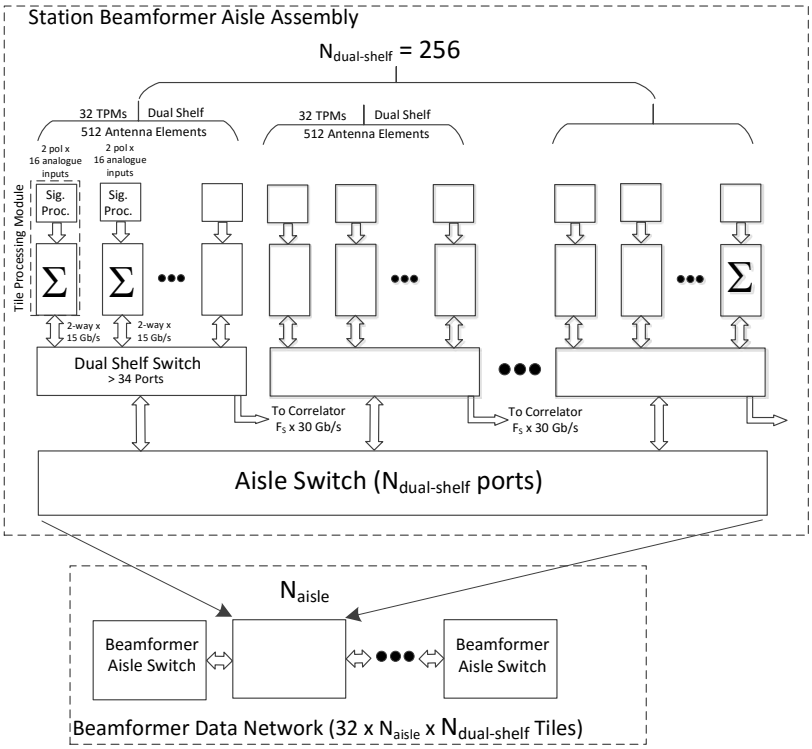

Figure 5: The station beam-former architecture illustrating a hierarchical arrangement of switches.

5.6.3.3 Data Rates from Clusters

The potential data rates from clusters is derived from the number of beam-sums produced in the cluster of six stations and the bandwidth per beam-sum. For the basic case of one beam per station for all stations, this is simply 6 x 11.4 Gb/s (see Section 5.6.2.3). In other situations the cluster data rate depends on the number of sub-stations allocated to each of the cluster stations. In section 8.2.1, four scientifically-useful cases are developed; these are used in Table 1 (cases 1-4) to provide illustrative data rates from clusters. A case from Table 2 for which the entire array is sub-divided into 7 sub-stations per station is also included.

Table 1: Data Rates Produced from Clusters (single beam)				
	Total No. Beamsums (N_s)	No. Beamsums per Cluster	Bandwidth MHz	Data Rate Gb/s
Basic	512	6	300	68
Case 1	1024	4	76	12
Case 2	1024	4	76	12
Case 3	2048	24	19	17
Case 4	2048	18	19	13
All-subs	3584	42	6.2	10

In Table 1 it is assumed that only the bandwidth required for each case will be transmitted to the Central Processing Facility (see Figure 3 and Table 2). Because the capacity of the correlator limits the bandwidth and the Correlator Performance Product (see Section 5.7.1) is proportional to N_s^2, the data rate transmitted from clusters need never be higher than for the basic mode of operation.

Because of the Diophantine nature of digital transmission over fibre, it is likely that combinations up to 100 Gb/s will be possible, which would leave room for more bits/sample, should that be necessary. This should be a subject of the cost analysis suggested in Section 5.6.1.

5.7 Correlator Architecture

Paralleling the approach in Section 5.6, a method is developed to assign as much flexibility of usage to the correlator architecture without significantly changing its overall cost. Assumptions and approximations are needed, designed to capture the overall performance of the correlator system as it is currently designed and costed, but which may not precisely mirror the current design in detail.

5.7.1 Correlator Performance-Product

- The correlator cost and size is determined mainly by the product of the number of baselines, the number of beams and the processed bandwidth.
- By design the maximum number of channels, $N_{fc\_max} = 2^{16} = 65536$.[11] The current correlator design is based on a single beam and 512 correlatable entities (stations).
- Thus 'Correlator Performance-Product' is: $P_{corr} = r_b \frac{N_s^2}{2} N_b N_{fc} \frac{300}{65536} = 1.5\ x\ 10^9$ Mb/s.
- The theoretical maximum number of stations, based on a single beam and a single coarse channel (0.781 MHz or $N_{fc\_max}/N_{cc\_max} \cong 171$ fine channels) is 10058. This and more reasonable bandwidths for representative numbers of correlatable entities (CEs: stations or sub-stations) are contained in Table 2. All of the combinations shown in Table 2 can be supported by the beam-former and correlator.
- The most scientifically useful modes in Table 2 are modes 1 to 4. Mode 4 permits the correlation of an almost full array of sub-stations, but allows only ~8 MHz of bandwidth for a single observation. Mode 2 is likely to be the best combination of numbers of sub-stations and bandwidth in the list.
- Examples of results of optimised placement of sub-stations for modes 2 and 3 are explored in Section 8.
- Many other combinations are possible and could be used for actual observations, including 'mixed' modes in which both stations and sub-stations are correlated.

Table 2: Bandwidth and Number of Beams for Given Number of CEs

Mode	N_s	N_{fc}	Total BW (MHz)	N_b	
1	512	65536	300	1	Stations only as CEs.
2	1024	16491	76	1	2^{10} CEs.
3	2048	4123	19	1	2^{11} CEs.
4	512 x 6	1832	8.4	1	Conservative 10-m CEs.
5	512 x 7	1346	6.2	1	Max. number of 10-m CEs.
6	10058	171	0.78	1	Max. number of CEs.

5.7.2 Integration/Dump time

- This could be a limitation on the correlator and will certainly have an impact on data transport and the science data processor.
- A simplified form is: $\tau_i = d/(2k_N B_{max} \Omega_E)$, where τ_I is the integration time, *d* is the diameter of the aperture, *B* is the longest baseline, Ω_E is the rotation rate of the Earth (7.2 x 10^{-5} rad/s).

[11] Because of oversampling and edge effects, this is likely to be fewer.

The formula is based on the amount of time it takes the aperture to rotate through half its width when tracking a polar field (approximately Nyquist sampling of the aperture). k_N is a factor to account for multiples of the Nyquist rate to account for time smearing, and also to account for fields-of-view larger than the θ_{FWHM}. Thus k_N is ~2 to remove time smearing; the radius of the second zero for a 'pill-box' aperture is ~$2\theta_{FWHM}$ (another factor of 2) so that k_N should be ~4. With B_{max} = 65 km; d = 35 m, $\tau_i \cong 1$ sec for the longest spacing.

- This can be scaled for shorter baselines (e.g. the core) or smaller apertures (e.g. 10 m instead of 35 m).

5.7.3 Correlator Output Data Rate

- The correlator will output $D_v = 2\frac{N_s^2}{2} N_{b-c} \frac{P}{\tau_i}$ real visibilities/sec, where the factor of 2 is for complex numbers, $N_{b\text{-}c}$ is the beam-channel product, N_s is the number of stations, P is the number of polarisation products (4) and τ_i is the integration time.
- Substituting for τ_i to yield full dependency on station size: $D_v = 2N_s^2 P N_{b-c} k_N \Omega_e \frac{B_{max}}{d}$.
- In terms of data-rates for 512 35-m diameter stations[12], $D_{out} = b_v D_v$, b_v is the number of Bytes per real-visibility, currently expected to be ~5. Thus D_v = 74 x 10^9 real-visibilities/s, and D_{out} = 368 GB/s (2.9 Tb/s). This is a fixed value for all situations in which the Correlator Performance Product is maintained, including the cases listed in Table 2.

5.8 Science Data Processing

Although arguably science data processing should be analysed in detail, it is out of scope for this document. For the different science areas, data processing techniques will differ, but will not depend greatly on the details of the array configuration, except for imaging over the very large fields-of-view implied by sub-stations. Even the station field-of-view may be difficult. It is not the intention to discuss specific costs, except to note the d^{-6} cost-scaling described in [RD14] and other places, where d is the antenna or station diameter. A Point Spread Function (PSF) with low side-lobes will be very helpful in this regard (see Section 8.4).

Application of calibrations are also likely to be very compute intensive, especially ionospheric calibrations.

6 Evolution of the V4D Configuration

In the calibration consultation meeting, held on Feb. 25, 2016 [RD3] [RD4], a number of aspects of the V4D configuration, particularly concerning the distribution of antennas in the core and within each station location, needed to be changed. Most of these have already been noted above.

1. Stations of 35-40 m diameter are a good match to the science, and it is important to retain randomised positions of antenna elements within stations.
2. There is not a strong scientific case for a superstation (i.e., with a structured boundary), but there is a case for retaining the distribution of collecting area represented in V4D. Thus a randomised distribution of stations in the outer part of the array is suggested.
3. The distribution of stations in the core should be randomised.
4. A capability of beam-forming and correlating as many sub-stations in the core as possible is very important to EoR/CD power spectrum observations.

[12] N_s = 512, $N_{b\text{-}c}$ = 65536 (65536 channels, 1 beam), k_N = 4, B_{max} = 65000, d = 35, P = 4.

While item 4 could have a major impact on the entire system, items 1-3 do not represent major changes to the present set of design assumptions.

7 V5 Configuration

Figure 6 and Figure 7 show the Central Area (see Figure 1) of an array configuration consistent with Sections 5 and 6, which for the purposes of reference is called V5 and is described in detail in [RD13]. The outer spiral arms follow the locations contained in [RD2], and the configurations of the clusters of stations in each location are random. Key performance plots for the configuration are contained in Figure 8 and Figure 9.

Important characteristics of this configuration are:

- Individual stations are identical in outline, but sufficiently large to permit a random distribution of antenna-elements within.
- The size of stations is designed to support a field-of-view of approximately 20 deg^2 at a frequency of ~100 MHz.
- The distribution of stations is designed to provide a clean synthesised beam with very low sidelobes. This results from a random distribution of stations with a modest amount of taper.
- The size of the core is designed to provide high brightness-temperature sensitivity with modest resolution in the synthesised beam (~5-10 arcmin) in the mid-frequency range.
- The previously derived locations [RD2] [RD11] in the array beyond the core each contain a cluster of randomly arranged stations. This provides a small amount of diversity in the u-v plane and avoids commonality of side-lobe structure in the synthesised beam. No real improvement in diversity will occur in baselines to the core, but baselines to stations outside the core may slightly improve.
- The profiles of both collecting area and of visibility density are smooth and 'scale-free' (i.e., fall off exponentially in the plane of the array and in the u-v plane, respectively, outside baselines formed from the core – see Figure 8 and Figure 9).
- The previously derived locations [RD2] [RD11] provide good instantaneous u-v coverage[13].

[13] Triangles of 3 station locations at fixed radii have been rotated away from the regular spiral pattern to best utilise the azimuthal sampling opportunities afforded by the un-masked regions of the site. In this way, the radial distribution of sensitivity is unchanged as well as the equiangular symmetry of the *u-v* sampling.

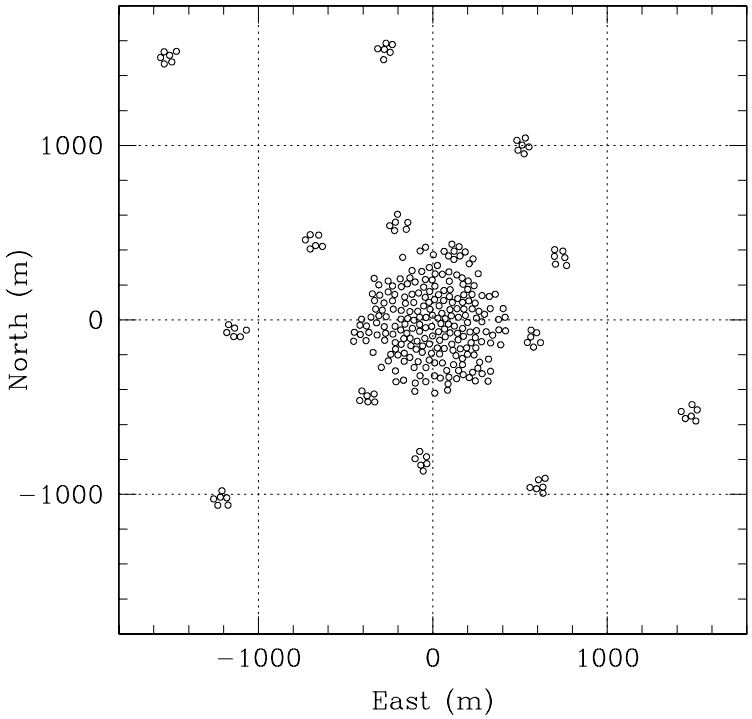

Figure 6: The central part of the V5 configuration. Each circle is a 35-m diameter station.

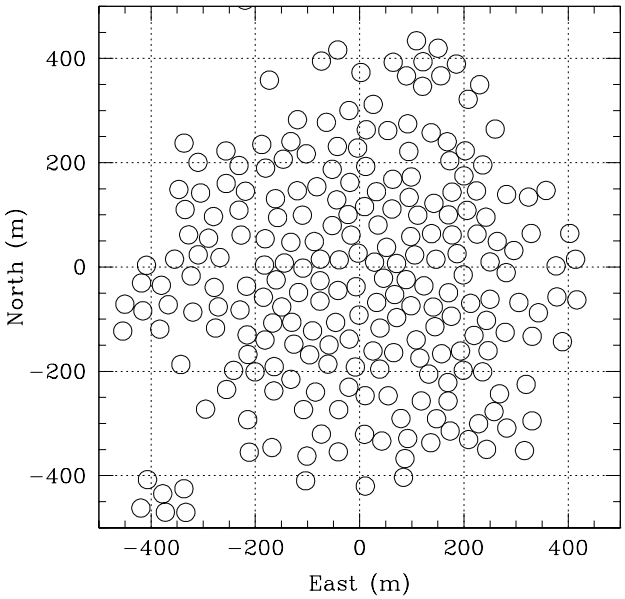

Figure 7: The core of the V5 configuration. Each circle is a 35-m diameter station. The cluster of 6 stations on the lower left is the second station cluster of the west spiral arm in Figure 6.

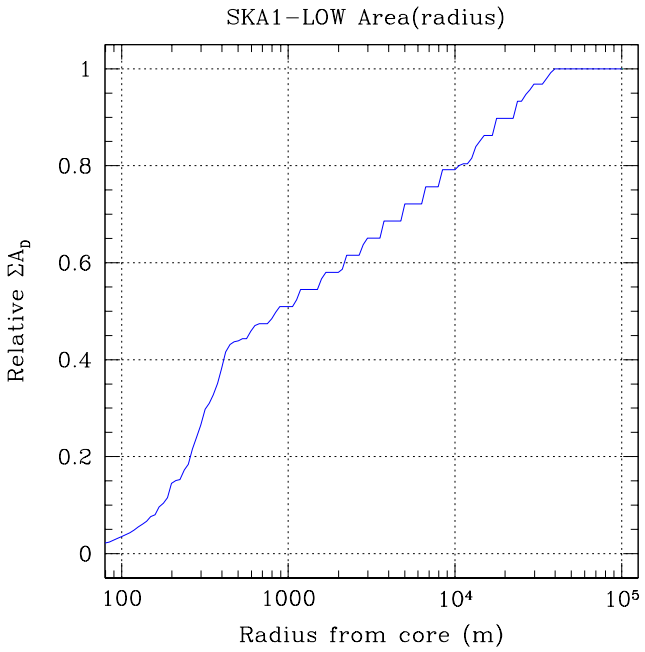

Figure 8: The radial profile of collecting area for the V5 configuration.

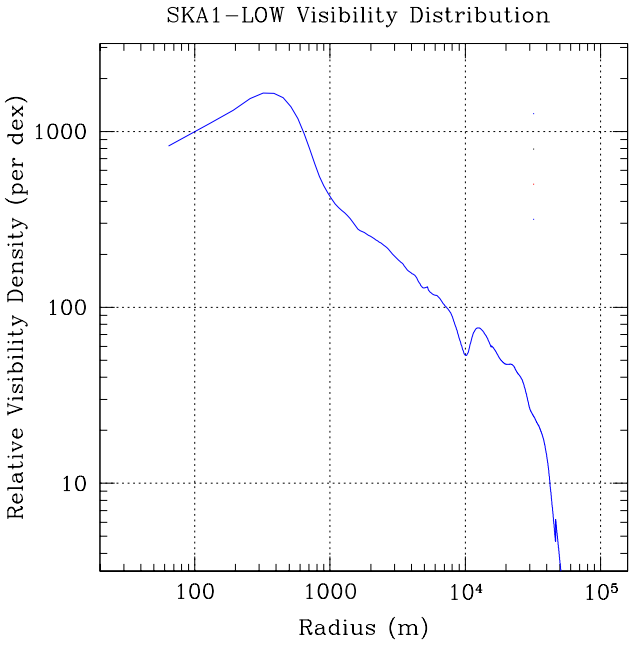

Figure 9: The radial profile of visibility-density in the u-v plane for the V5 configuration. This example is based on a ±2 hour track at a Declination of -30°, assuming a 30% fractional bandwidth.

8 Potential Observational Setups

8.1 Basic Setup – 512 stations

The most basic observation set-up is simply to beam-form each of the 512 35-m diameter stations. If the set-up is for one beam, the entire 300-MHz bandwidth is available. Otherwise the available bandwidth is 300 MHz, divided by the number of beams.

8.2 Variations Containing Substations

Table 2 contains values for the number of potential sub-stations for Modes 2 and 3, the implications of which will be explored in more detail in this section. This table, of course, does not define the section of stations to actually be correlated. The following are considerations for making such a selection, based on an array designed for EoR/CD observations (power spectrum and imaging):

- Because ionospheric calibration is required continuously, it is assumed that any distribution of collecting area must include stations or sub-stations at each of the locations in the outer elements.
- As completely filled a radial profile of visibility density as possible, down to spacings $\geq$10 m (see Sections 5.4.2 and 5.4.3).
- As much collecting area in the core as possible, moderated by obtaining a smooth radial profile of *u*-*v* visibility density, and by sufficient collecting area in the outer stations to calibrate the ionosphere.
- A variety of setups can be scheduled, provided that the station-channel-beam trade-space rules are obeyed.

8.2.1 Specific Substation Cases

Four representative variations are considered, all utilising the basic configuration illustrated in Figure 6 and Figure 7. These cases are all for fields covering $\pm$2 hr of Hour Angle, passing through the zenith.

1. 1024 sub-stations randomly distributed within stations.
    - Stations are populated with 4 randomly-located substations in the core and 4 randomly-located substations in one of the 6 stations at each cluster location.
    - 75 MHz of bandwidth is available.
    - Figure 10 shows the core area for this case.
2. 1024 sub-stations regularly distributed within stations.
    - Stations are populated with 6 substations in the core and 4 substations in one of the 6 stations at each cluster location.
    - 75 MHz of bandwidth is available.
    - Figure 11 shows the core area. Figure 12 shows a 4000-m sized area, which indicates the transition from 6 to 4 sub-stations.
3. 2048 sub-stations randomly distributed within stations.
    - Stations are populated with 4 randomly located substations in all of the 512 stations.
    - 19 MHz of bandwidth is available.
    - Figure 13 shows the core area for this case.
4. 2048 sub-stations regularly distributed within stations.
    - Stations are populated with 6 substations in the core and 6 substations in 3 of the 6 stations at each cluster location.
    - 19 MHz of bandwidth is available.
    - Figure 14 shows a 4000-m sized area, which indicates the population of stations outside the core for this case.

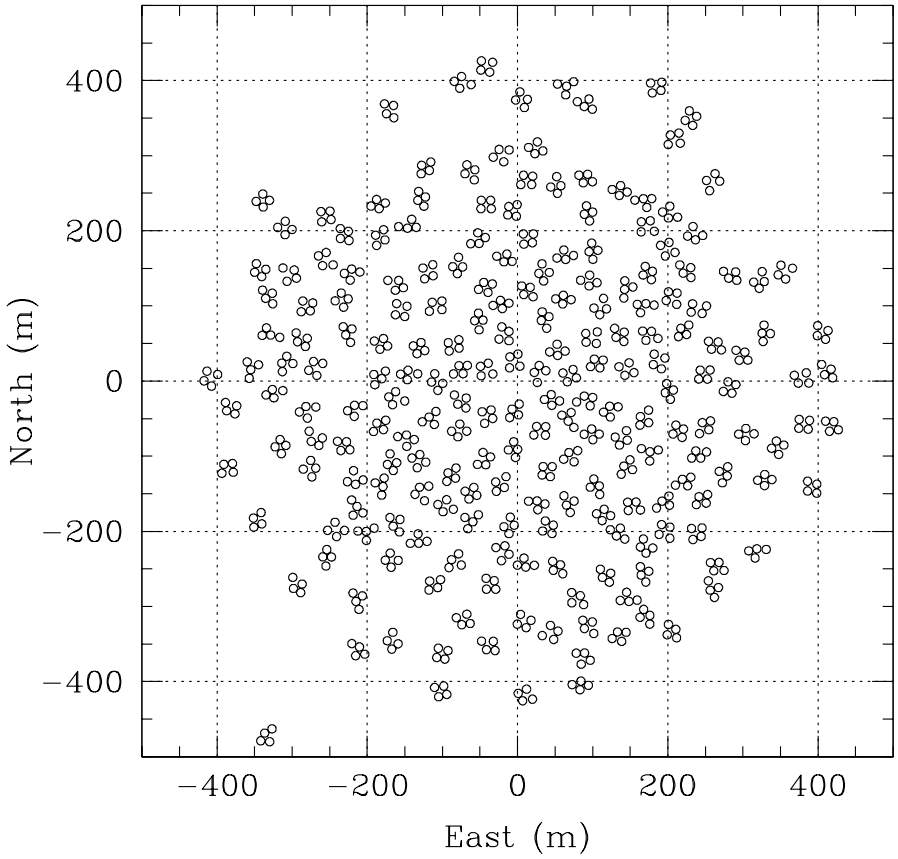

Figure 10: The core area for Case 1.

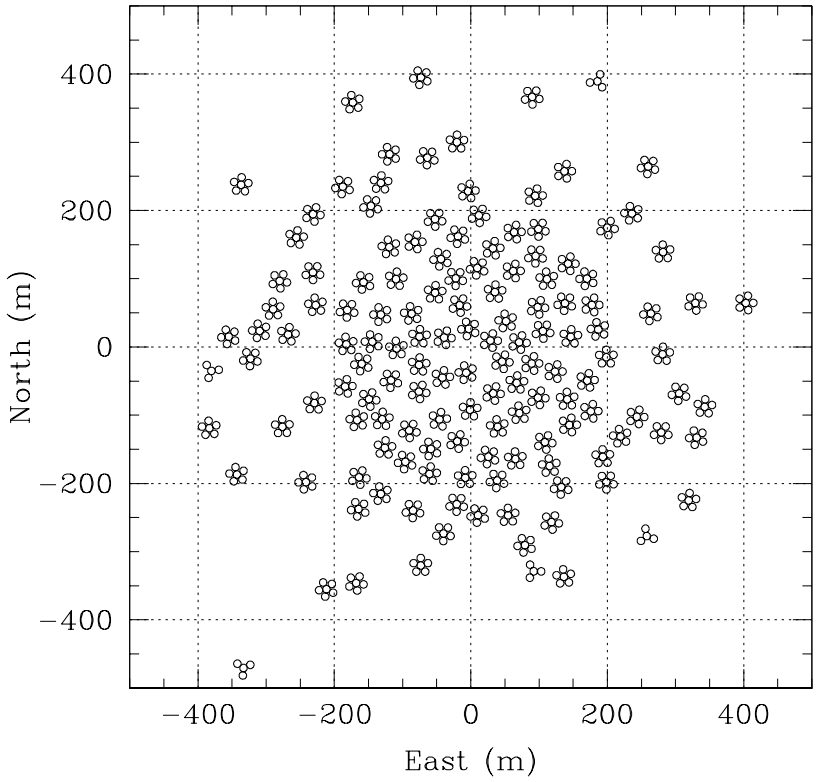

Figure 11: The core area for Case 2.

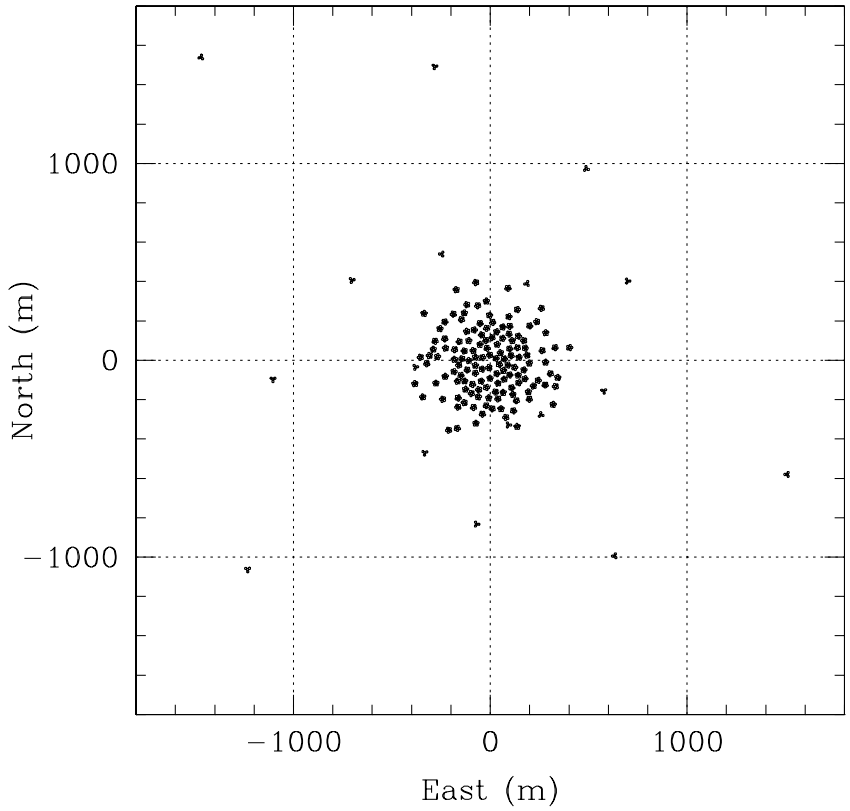

Figure 12: The 4000-m scale for Case 2.

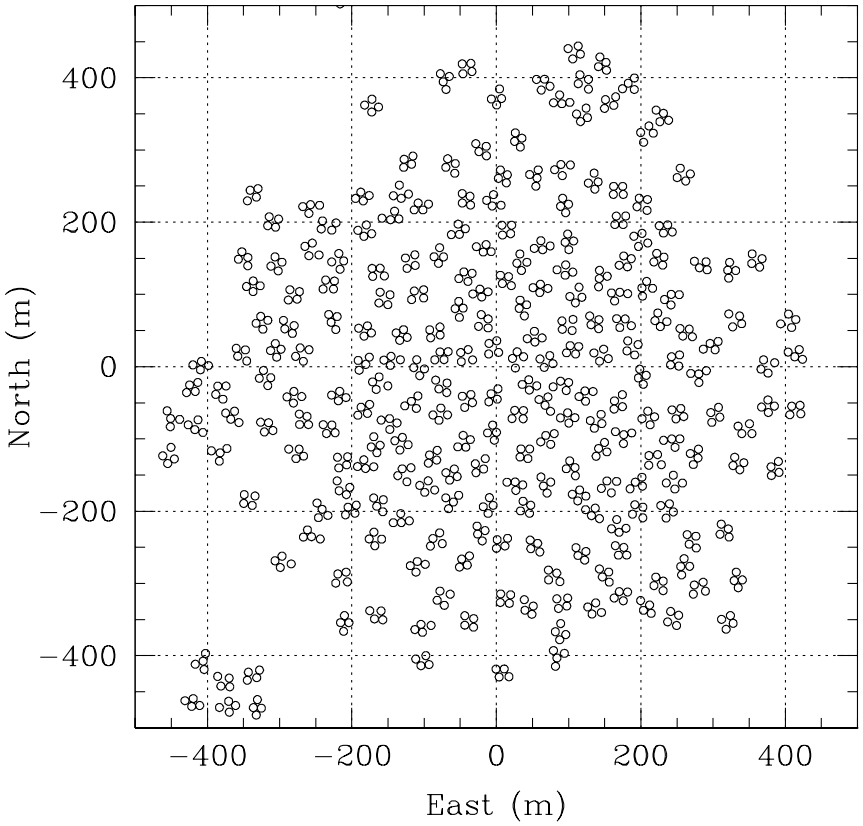

Figure 13: The core area for Case 3.

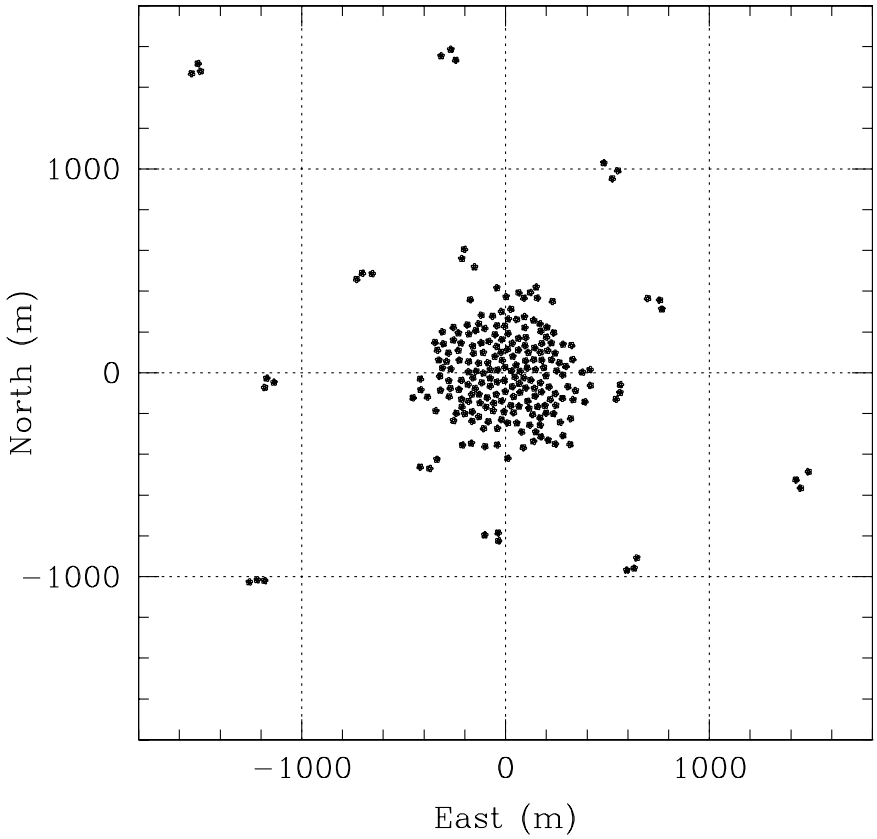

Figure 14: The 4000-m scale for Case 4.

8.3 Coverage of the Central Part of the *u-v* Plane

As noted in Sections 5.4.2 and 5.4.3, very short spacings (low spatial frequencies) are needed for EoR/CD imaging and power spectrum observations. Also Section 5.5.3 notes the motivation for imaging very diffuse objects, covering wide fields.

Figure 15 is a log-plot of relative visibility density out to a radius of ~500 m for the four exemplary cases described here. The ideal profile is a smooth, flattish curve beginning at the smallest radius possible, continuing out to the edge of the core and then falling off exponentially from there.

This plot shows that with 11-m diameter stations that the density of visibility measurements extends to less than 10 m. Below 30 m there are both peaks and dips present, but there are no actual gaps. All the features present will be smoothed and modified by both projection effects when the field is off the zenith and by gridding effects. Projection effects will increase for fields that do not pass through the zenith, resulting in a smoother profile for those pointing directions. All of the structure in the profile is related to characteristic scales imprinted by the size and spacings present in Figure 6 (35-m diameters) and in figures for the sub-station cases (e.g. Figure 11 and Figure 13, 11-m diameters).

All of the cases show the dip at ~25 m. This is likely related to the 35-m scale, in which distance between substations can occur less frequently than other characteristic distances, modified by projection effects. The randomised cases show a smoother profile from ~9 to ~20 m than the regular cases.

Note that these are examples of substation allocations; they are not 'built in' to the design, and the allocation can be optimised within the trade-off limits to fit the science goals of the observation.

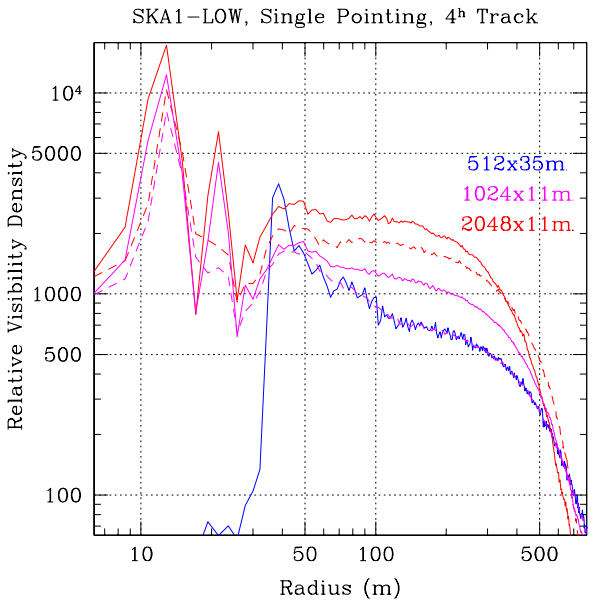

Figure 15: A comparison of visibility density plots for the four cases and the 36-m diameter station case. The regular substation cases are shown as solid lines; the random as dashed lines. The solid blue line, for the full array of 35-m stations is shown for comparison. In all cases the plot is a tangentially integrated profile over ±2 hours of Hour Angle, passing through the zenith.

8.4 Quality of the Point Spread Function (Beam)

The quality of the point spread function (PSF) is characterised here using three measures at the fiducial frequency of 140 MHz:

1. The ratio of noise on an image to the minimum attainable (with natural weighting);
2. For a ±2 hour track in Hour Angle passing through the zenith, the ratio of the rms side-lobe level to the peak of the synthesised beam in an area 10 x 10 beam areas in size;
3. Same as item 2 for a snapshot at the zenith.

Figure 16 contains plots in order from bottom to top of these measures for continuum observations, where continuum is taken as $\Delta f/f = 30\%$. Figure 17 plots the same things for a single frequency. In both cases they are plotted against beam-size from ~5 arcsec to ~1.7°.

Taken together with Figure 8 and Figure 9, these figures illustrate that this array configuration provides the qualities described in Sections 5.4 and 5.5 for the scope described in Section 1.2. In addition the ability to utilise sub-stations provides direct measurements of very short spacings (Figure 15).

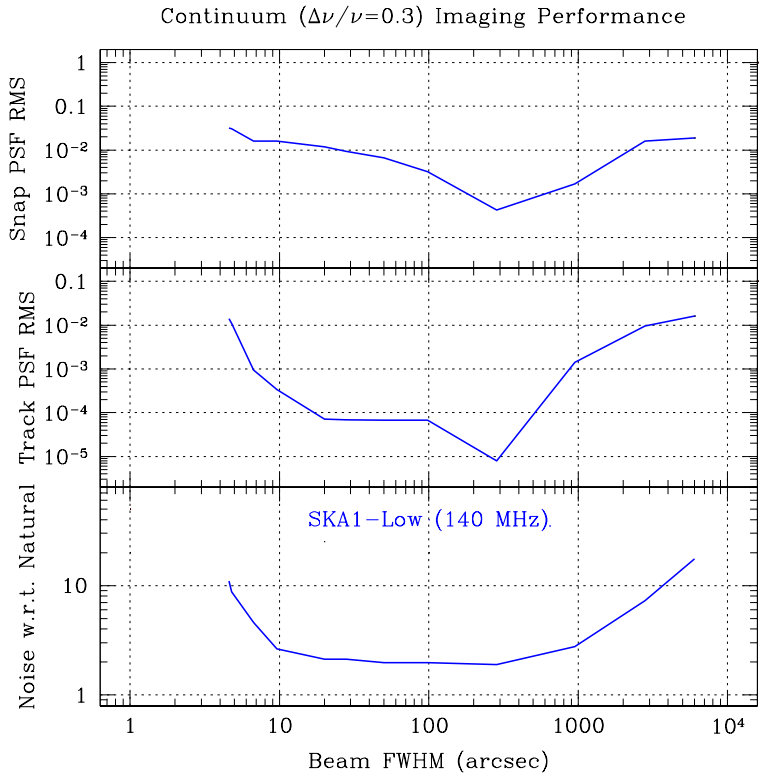

Figure 16: Characterisation of the continuum PSF for the V5 configuration using three measures of performance described in the text.

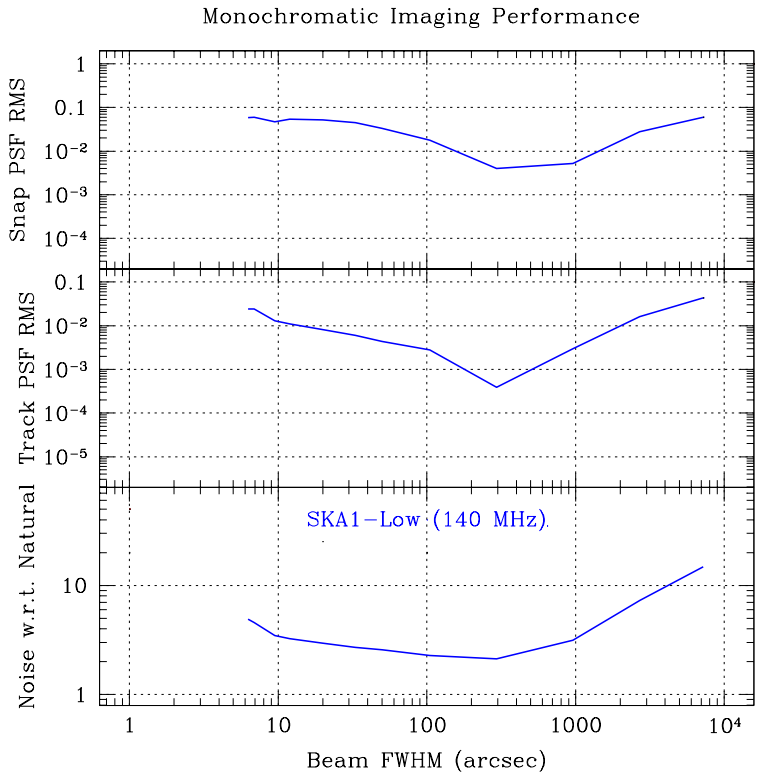

Figure 17: Characterisation of the monochromatic PSF for the V5 configuration using three measures of performance described in the text.